Analysis of the Capacity of Radar Time Series Data for Crop Mapping in the Context of the Sahel: Case of Groundnut, Millet and Maize in Senegal

Gayane FAYE[1], Fama MBENGUE[1], Mamadou Adama SARR[2,3], Mamadou MBAYE[4], Lacina COULIBALY[5], Modou MBAYE[1], Abdou Ka DIONGUE[4]

[1]Laboratoire de Télédétection Appliquée/Institut des Sciences de la Terre / Cheikh Anta DIOP University of Dakar (LTA/IST/UCAD), SENEGAL. gayane.faye@gmail.com

[2]Centre de Suivi Ecologique (CSE) of Dakar, SENEGAL.

[3]UFR-Université Gaston Berger de Saint-Louis

[4]Laboratoire d'Études et de Recherche en Statistique et Développement/UFR de Sciences Appliquées et de Technologie/ Département de Mathématiques Appliquées/ Université Gaston BERGER of Saint-Louis, Senegal.

[5]Laboratoire de Géomatique Environnementale, École de foresterie, Université de Moncton, Nouveau-Brunswick, Canada.

Abstract— Monitoring agricultural areas, using remote sensing, has been a major issue in the Sahel region, due to the small size of farm plot compared to satellite spatial resolution. The main goal is to develop a methodology based on radar data for mapping crops in Senegal. Training plots were used to analyse temporal dynamics of radar signals. The result shows that the possibility to separate agricultural area from other land cover at the beginning of the rainy season. The radar signal of the three crops are confused at the beginning but we note a strong difference at the end of the growing season, where peanut crops signal is marked by a sharp fall. Variance analysis allowed to select images which are able to discriminate these cultures.

The Classification And Regression Trees (CART) model used is able to identify peanut plots with more than 82% of accuracy, but confuse maize crop (accuracy less than 70%). This result means the resulting inability to separate the two types of maize crops (one which is sown early and harvested in mid-season, another sown in mid-season and harvested at the end of the season). So, in this area, the use of radar permit to improve crop mapping considering agricultural practice of cereals.

Keywords— Remote Sensing, Synthetic Aperture Radar, Sentinel-1, Agricultural monitoring areas, Senegal, Nioro.

I. INTRODUCTION

The use of earth observation data for vegetation monitoring and agriculture has been the subject of many research projects in the past [1]. More recently many scientists have demonstrated the potential of remote sensing as a robust method for monitoring agriculture [2, 3, 4, 5, 6], and for better dealing with the impact of climate change in this vital sector of the nation's economy.

In the Sahel region, where agriculture is still highly dependent on rainfall (for example, less than 5% is irrigate in Senegal for example), which make it very vulnerable,

particularly in the context of climate change. This situation has serious food security, economic and social impacts. In addition, reliable data and information is not always readily available to help better anticipate sound practices that could improve agricultural productivity. Thus, it is urgent to build tools and methods that could improve the accuracy of agricultural data and statistics, for better management of this sector and thus, contribute to fight against food insecurity in this region. However, remote sensing applications in the Sahel region can be very challenging, as the agriculture system is often dominated by small plots of lands (generally less than 2 hectares) with mixed crops,

making difficult to differentiate unambiguously and map the different crops; and thus, estimate routinely yield from a remote sensing approach.

The objective of this study is to exploit the potential Radar Sentinel-1 times series data for mapping agricultural area in Sahel context.

These studies have shown strong correlation between the spectral reflectance of crops at certain wavelengths and their physical and biological characteristics, thus demonstrating the possibility of using satellite images as a tool for monitoring the state of crops. However, in the Sahelian context, the differentiation of crops with remote sensing has not been easy because of the small size of plots (typically 2 ha) compared to the spatial resolution of the sensors. However, the advent of new generations of optical and radar remote sensing images with better resolutions (high spatial, spectral and temporal resolution) provides new options for mapping agricultural production.

In this study, we used the temporal variability of Sentinel-1 radar signals (C-band, VV and VH polarisation) during the agricultural season to try to discriminate millet, maize, and peanut crops at the scale of the plot. The use of radar imaging is preferred as optical data are sensitive to cloud cover during the rainy season in Senegal (July to October).

Analysing the temporal variation of the signals of different crops in VV and VH polarisation can be useful in distinguishing between them as these crops do not have the same phenological cycles [7, 8, 9]. Hence this analysis seeks to identify the periods when the greatest differences between crop signals is noted. It is also possible to use the signals of different types of land use to create a mask map of non-agricultural areas.

Several authors [10, 11, 12, 13, 14, 15, 16, 17, 18] have demonstrated that the monitoring and mapping of herbaceous vegetation by radar methods is difficult due to the sensitivity of the radar signal to various surface parameters (soil roughness, soil moisture and vegetation). However, with some vegetation covers, the contribution of the soil varies with time and becomes minimal compared to that of vegetation and so temporal monitoring throughout the agricultural season suggest that it is possible to overcome this limit.

II. MATERIALS AND METHODS

Study area

The study area is located in the "peanut basin" which covers a large part of central Senegal. Annual rainfall ranges between 700 and 1100mm, and agriculture is mostly made of millet, maize and peanut which is the main source of income for the population [19].
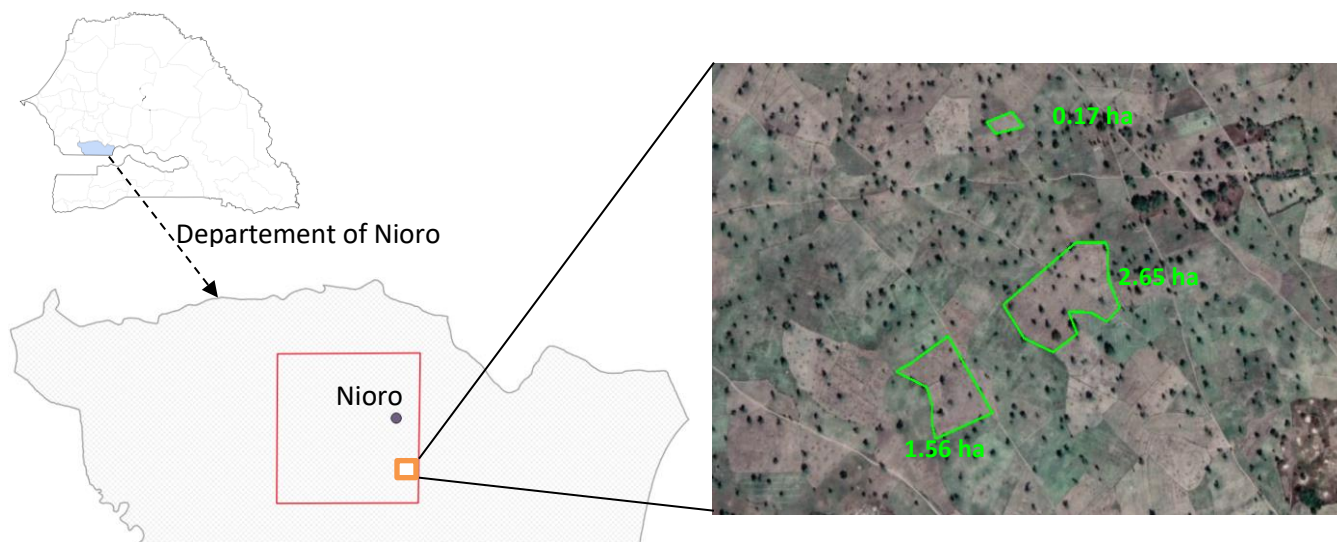

Fig.1: Location of study area

Field data

The three crops targeted in the current study have the following major characteristics:

(i) Millet is an herbaceous cereal with a phenological cycle of 75 to 90 days and height at maturity of 220 to 250 cm [20, 21, 22, 23];

(ii)   Maize is an herbaceous cereal with a phenological cycle of 75 to 80 days reaching 175 to 200 cm at maturity [24, 25];

(iii)   Peanut is a creeping legume with a cycle of 90 to 120 days and height at maturity of 30 to 70 cm [26, 27].

In total, an in-situ database of 150 control plots (50 per crop) was set up to serve as a training and validation data. The data were collected during the field work using a GPS to digitize the geographical boundaries of the plots. To avoid edge effects and eliminate mixed pixels between adjacent crop plots, contour boundaries were adjusted using GOOGLE EARTH.

III.   DATA AND METHODS

C-band sentinel-1 (SAR sensor) data are used. This data has 10 meters of spatial resolution in two polarizations (VV and VH) and temporal repeatability of 12 days. A total of 14 images of the area were obtained from the ESA website [28] for the period of June to December 2016. These were downloaded and corrected for geometric distortions (geocoding, georeferencing), and then filtered to reduce speckles. The data were normalized (radiometric calibration) to transform the backscattered signal (Digital Number) into backscattering coefficient $\sigma °$ (in dB), a quantity proportional to the ratio of received signal power and transmitted signal power by the antenna [29].

The first step was to extract the pixel values of the control plots for all selected and corrected images, and to analyze them in order to identify the best combinations able to discriminate the three crops.

(a) Extraction of pixel values of the control for all images: After adjusting the boundaries of the control plots, and correcting the radar data, pixels values of all control plots of the images (from June to December) were extracted.

(b) The second part is the analysis of the temporal signal of agricultural and non-agricultural areas. This was to create a mask of non-agricultural areas and focus on the cropped areas.

(c) Comparison was made of the temporal evolution of crops signals during their different phenological phases in both polarisations, with the aim to identify the most discriminating periods.

(d) In the following step, an ANOVA (Analysis of Variance) was performed in order to select the data having the capacity to discriminate the three cultures (millet, maize and peanut). The ANOVA was used to compare the mean of the signal in pairs for each polarization at each date. For each image (date), when the p-value was higher than 0.05, we concluded that the two crops signals were not different. Then, a check was made with the confidence interval around the difference. For each data, when the confidence interval included the value of zero (max positive and min negative), the data was deemed not able to discriminate crops, then it was excluded.

(e) In the last step, a CART (Classification And Regression Tree) was done on the selected data by the ANOVA. The general principle of CART is to recursively partition the input data (pixel value) in a binary way, then to determine an optimal sub-partition for the prediction [30]. Also, CART is a classification method that uses in situ data to build a descriptive and predictive model of a relationship between a set of predictors and a categorical variable [31]. Here 2/3 of the data were used to build the CART model and the remaining 1/3 was used for the validation, thus making it possible to calculate the confusion matrix.

IV.   RESULTS AND DISCUSSIONS

a-   Maps of agricultural areas

The first task was to analyse the signals of the different land covers in order to mask the non-agricultural zones. Figure 2 shows significant differences between the different types of land use, especially at the beginning of the rainy season (June 29, July 23), where signals from agricultural areas stand out from those of others (habitat, water and natural vegetation). VV polarization is more useful in this regard than VH polarization. There was also a seasonal sensitivity of the vegetation to the radar signal, with the maximum sensitivity in the middle of the season corresponding to the peak of growing season for vegetation (when plant content is high). This consistent with results obtained over the entire Sahelian band where the C-band signal is very sensitive to seasonal dynamics [13, 14, 15, 32, 33, 34].

Images of June 29 (in VH) and July 11 (VH and VV) provide the greatest differentiation of agricultural and non-agricultural zones and so these were combined to create a mask of non-agricultural areas by using a supervised classification.
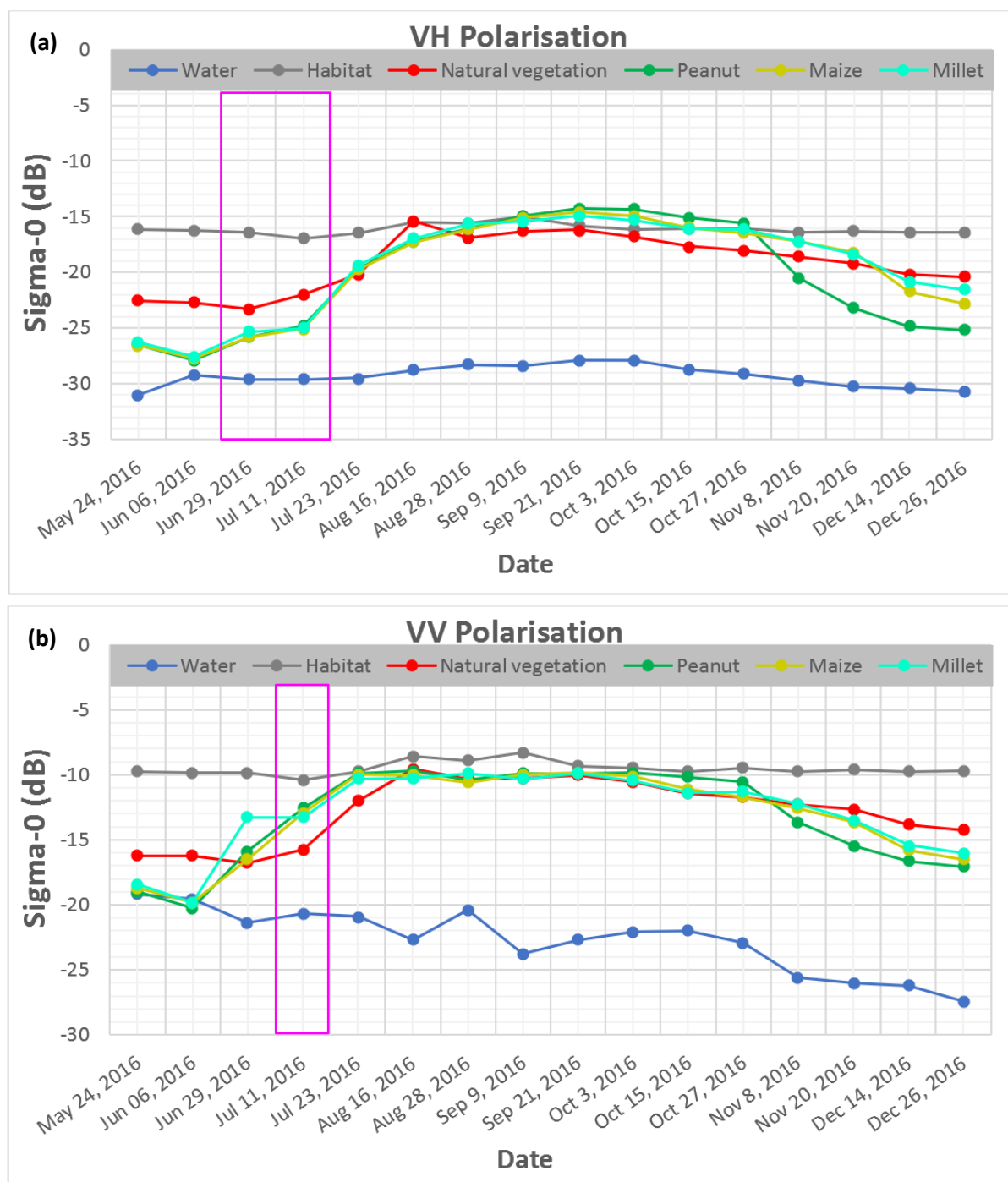
Fig.2: Temporal variation of the signals of the different land uses in VH (a) and VV (b) polarisation

The color composition in "false color" of these three images (VH of June 29, VH and VV of 11 july 11) in Figure-3 showed significant differences between agricultural and non-agricultural areas. The density curves of different land uses (Figure-3) showed the possibility to extract agricultural areas. Indeed, in polarization VH (June 29 and July 11) water areas mixed slightly with agricultural areas. However, the polarization VV (Figure-3) allowed the separation of the different classes.
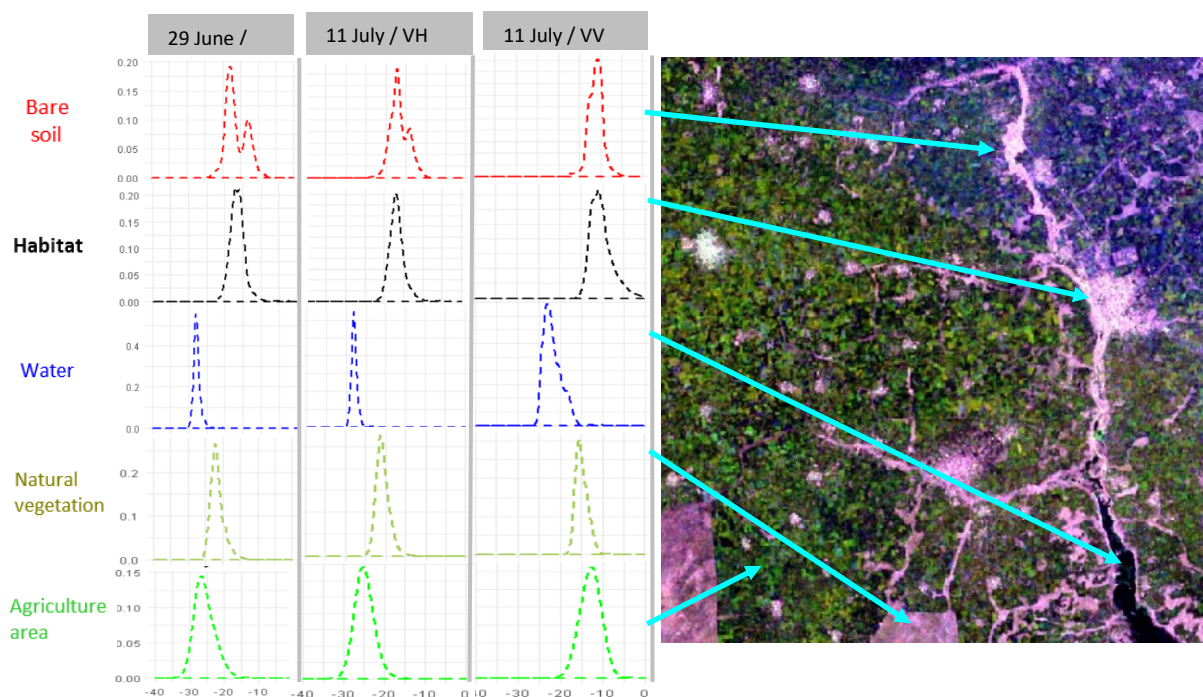
Fig.3: Colored composition and density curves of the different land cover and color composit of the images of June 29 (VH) and July 11 (VH and VV)

Figure 4 shows the resulting mask map of agricultural, non-agricultural and water areas (with a Kappa coefficient of 0.91). All subsequent analysis was limited to the agricultural areas.
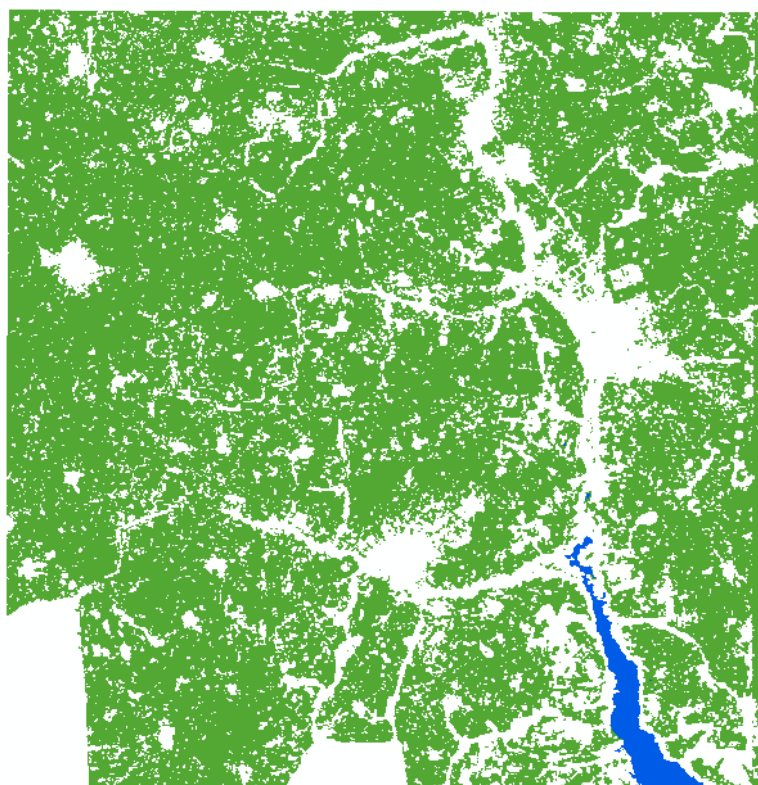

Fig.4: Agricultural areas (green), non-agricultural areas (white) and water areas (blue) .

b- Analysis of temporal signal of three crops (millet, maize et peanut) in VV and VH polarisations

The crop signals were strongly confused during the growth season under polarizations (Figure 5a and 5b), making it impossible to distinguish between these three crops. This happens because the C-band radar signal is sensitive to aerial vegetation as well as to physical surface parameters such as roughness and soil moisture [18, 17, 35, 36, 37, 38]. As a result, when vegetation cover was low, the soil contribution dominated in the signal [39], thus limiting the ability to differentiate crops.

Figure 5a and 5b show that crops signal varies respectively between -18 to -10 dB (8 dB amplitude) in VH polarization and -26 to 14 dB (12 dB amplitude) in VV polarization. This is perfectly normal because the Fresnel reflectivity coefficients governing the radar response depend on the polarization [11].

It was also observed that the signal in VH polarization reached its maximum value around the 200th Julian day corresponding to the 18th of July when the VV is at only half of its maximum value. This saturation of the VH signal at the beginning of the season shows a strong sensitivity of this polarization to the low vegetation cover.
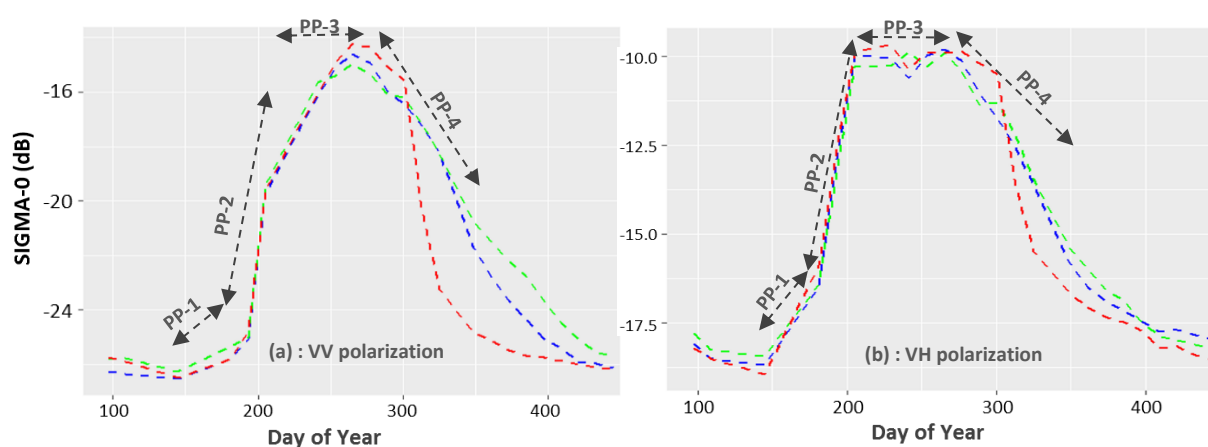

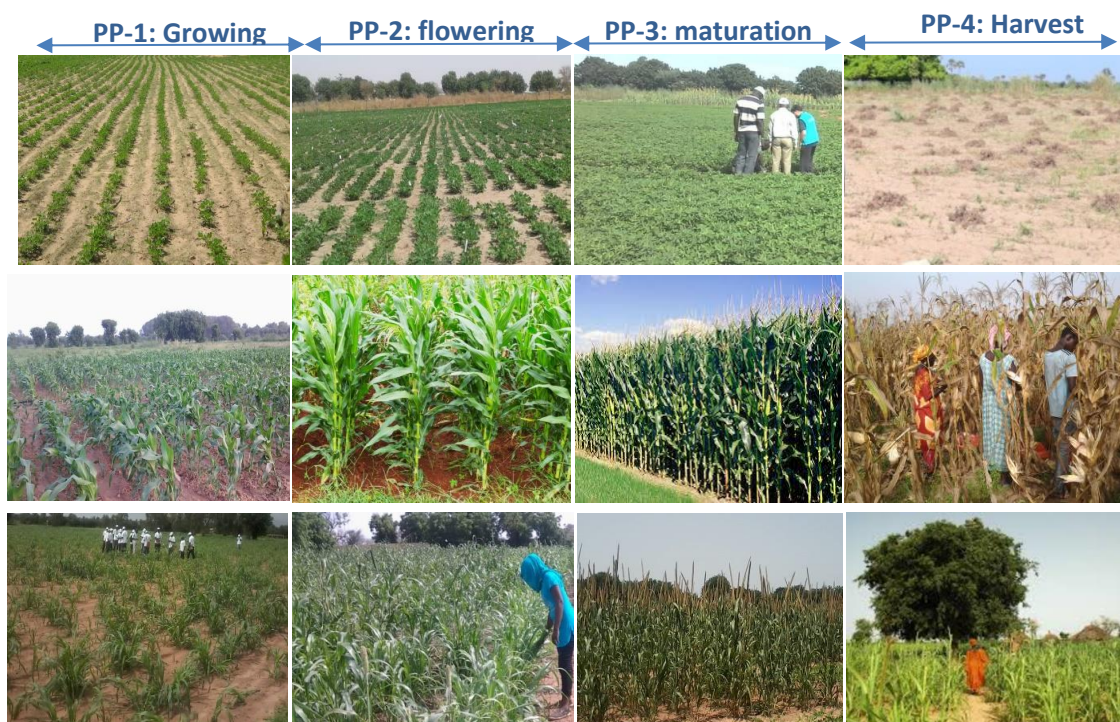*Fig.5: Peanut (red), maize (blue) and millet (green) during their different phenological phasis (PP)*

Fig.6: Photo of the three crops (peanut, maize and millet) during their different phenological phasis (Photo ISRA, Institut Sénégalaise de recherche Agricole)

A slight difference between the three crops in the VH signal was noted between the 200th and 265th day of year (July 18 to September 21) corresponding to the period of growth and maturation. After this period, the peanut signal remained high especially in VV polarization. This is because millet and maize reached their maturity more rapidly and they were being harvested, leading to a decline in their signals. However, the way that these two crops are harvested (cutting the ears and leaving the stems in place) makes their signal slowly decrease compared to that of the peanut where the harvest is done by cutting everything and leaving a bare soil (Figure-6). This explains the sudden drop of the peanut

signal, which was much more marked in VV polarization (Figure-5).

To better understand the noted differences, an analysis of the distribution of values is made for each date (Figure 7). It should be noted that for almost all the dates and for each polarization, more than 50% of the values were within a range of less than 3 dB, for all crops. On the other hand, the distribution was normal (on average the number of values above the median was equal to the number of values below). Thus, the distribution of values was not related to either the type of crop or the phenological phase.
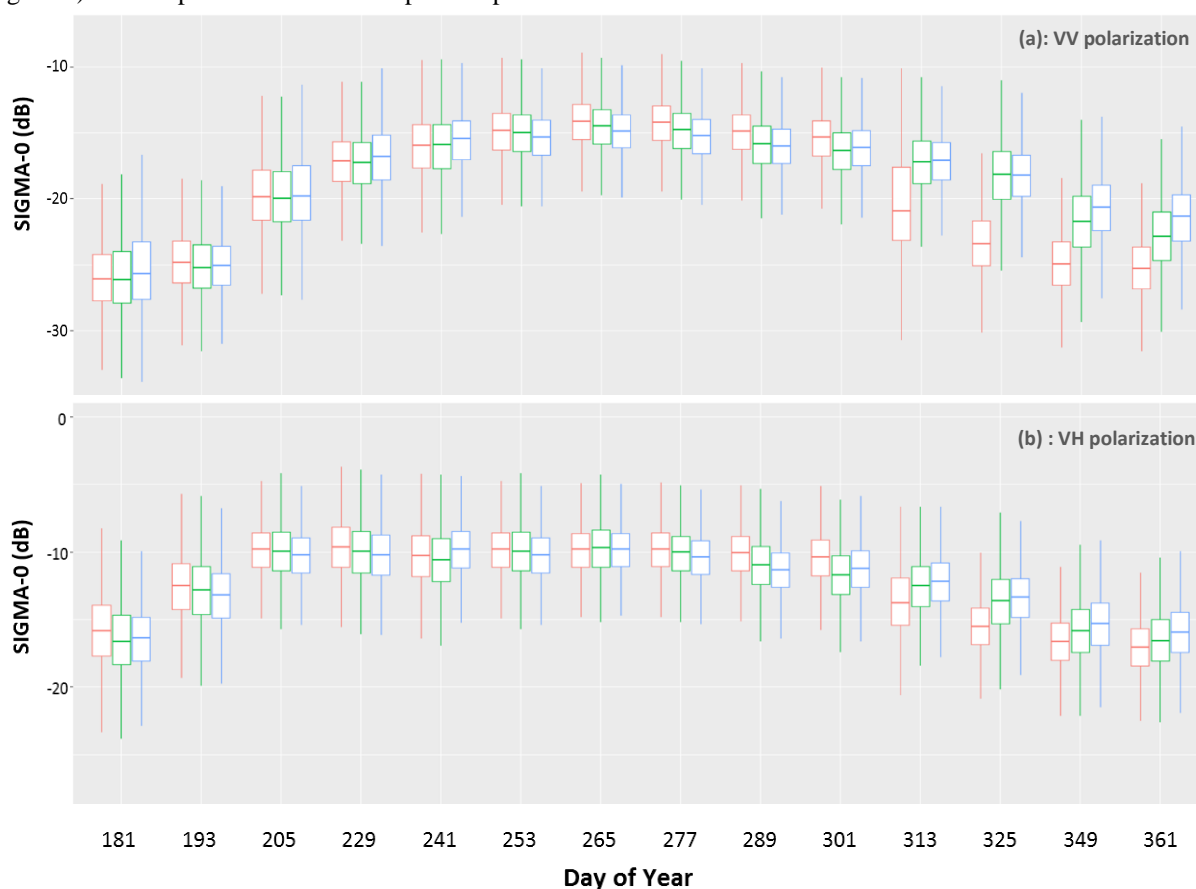

Fig.7: Distribution of radar signal (in VV and VH polarisation) of peanut (red), millet (blue) and maize (green) during the rainy season

c- ANOVA (Analysis of variance) of millet, maize and peanut signals in VH and VV polarisations

ANOVA identified dates to discriminate different crops. This part consisted in comparing crop reflectance values in pairs while calculating a coefficient of variation of the difference between crops signals for each date (Figure 8).

An image was discarded when the deviation around the variance between two crops contains the value zero, indicating that it is not possible to distinguish between the two crops for this date. Table-1 summarizes the results of the ANOVA with "1" for acceptable image and "0" non-discriminative image. In VV polarization, 12 variables were considered discriminating compared to 9 variables for VH.
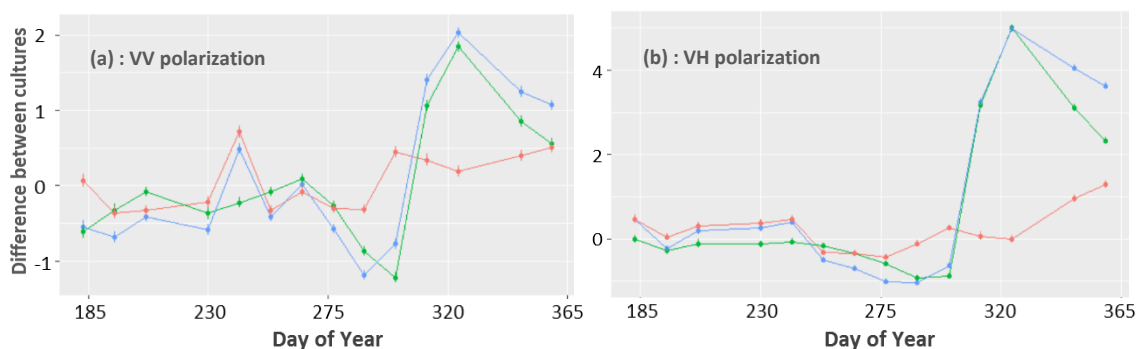
Fig.8: Confidence interval associated with the difference between different crops compared two by two for all dates (red: millet-maize, green: peanut-maize and blue: peanut- millet)

Table-1: Summary of the ANOVA result (1) for the optimal dates and (0) for wrong date (dat1, dat2… mean numero of the selected image)

Month	June	July		August		September		October			November		December	
Date	**29**	**11**	**23**	**16**	**28**	**09**	**21**	**03**	**15**	**27**	**08**	**20**	**14**	**26**
Day of year	**181**	**193**	**205**	**229**	**241**	**253**	**265**	**277**	**289**	**301**	**313**	**325**	**349**	**361**
VV	0	1	1	1	1	1	0	1	1	1	1	1	1	1
		dat1	dat2	dat3	dat4	dat5		dat6	dat7	dat8	dat9	dat10	dat11	dat12
VH	0	0	1	1	0	1	1	1	1	1	0	0	1	1
			dat1	dat2		dat3	dat4	dat5	dat6	dat7			dat8	dat9

d- Classification and regression trees (CART)

In the CART model, the type of crop is the predicted variable, using reflectance values resulting from the selected images (explanatory variables). In addition to the first selection made from the ANOVA, the CART itself selects the best images (i.e. dates) to separate crops.

(i) VV polarization (Figure-9): the explanatory variables selected by the CART, allowing the best differentiation of the three cultures, were the reflectance of the images of 23th of July (dat2), 28th of August (dat4), 15th of October (dat7) and 20th of November (dat10).
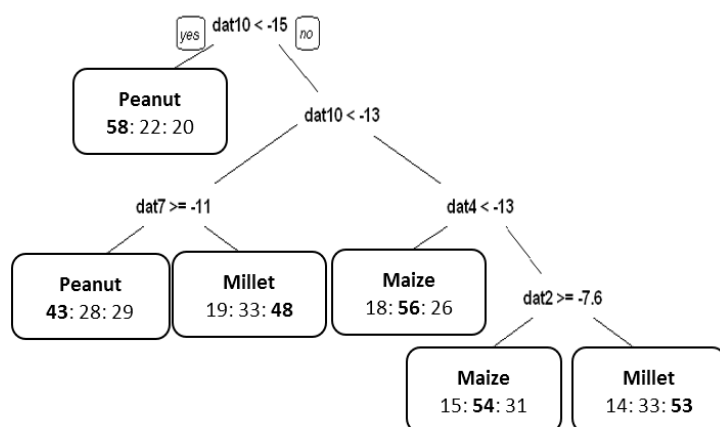
VV Polarization

	Peanut	Maize	Millet	Error %
Peunut	83.2	2.8	14.0	16.8
Maize	48.7	11.4	39.9	88.6
Millet	40.9	5.6	53.5	46.5
Global error = 47.3%				

Fig.9: Graph of CART result (in %) and confusion matrix (VV polarisation)

(ii) VH polarization: There were 9 explanatory variables but the model selected only three images: 27th of October (dat7), 14th of December (dat8) and 26th of December (dat9). The evaluation of the confusion matrix obtained from the VH data yielded a global classification error of 40.8% with still a high confusion for maize (Figure-10).
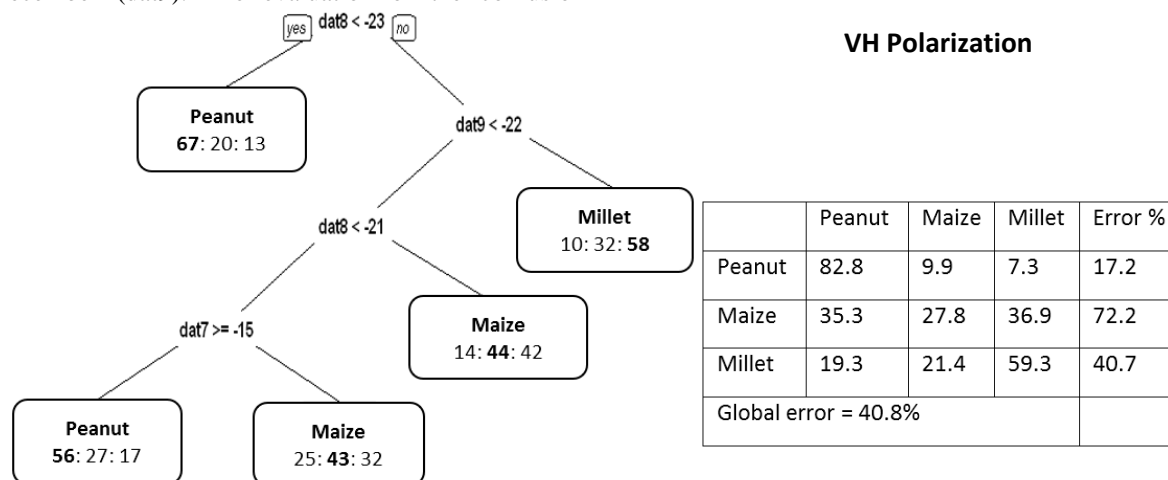
VH Polarization

	Peanut	Maize	Millet	Error %
Peanut	82.8	9.9	7.3	17.2
Maize	35.3	27.8	36.9	72.2
Millet	19.3	21.4	59.3	40.7
Global error = 40.8%				

Fig.10: Graph of CART result (in %) and confusion matrix (VH polarisation)

The evaluation of the two confusions matrix shows a very good recognition for peanut with an error of 16.8% in VV and 17.2% in VH polarisation (Figures 9 and 10 respectively). This is because the behavior of the peanut, with respect to the radar signal following the two polarizations, is different from that of the two other plants. Indeed, the size of the peanut plant rarely exceeds 50 cm while the others are more than one meter high. On the other hand, harvesting of a peanut field results in bare soil, unlike the other two crops where stalks remain after harvest of the ears before slowly decaying (Figure-6).

There was strong confusion for maize under both VV and VH polarisation with maize being incorrectly classified as peanut (48.7% error under VV and 35.3% under VH) and as millet (39.9 % under VV and 31.9% under VH), with a global error of 88.6 % (VV) and 72.2 % (VH). This strong confusion results from the fact that in this part of Senegal, there are two types of maize crop. Commercial maize is planted at the beginning of the rainy season and harvested in September. The fields are then often ploughed again and replaced by watermelon which is a creeping plant with a morphology identical to that of peanut and harvested at the same time as peanut. The second type of maize crop is used for food; it is sown later (mid-August) and harvested at the same time as millet. These two reasons explain the strong confusion noted for maize plots. To improve accuracy in maize discrimination, it is necessary to differentiate between the two types of maize in the sample.

Millet performs better with an overall classification error of 40.7% in VH and 46.5 in VV, indicating that millet discrimination is independent of polarization. However, VH polarisation proves better at distinguishing between millet and peanut, with only 19.3 % error compared to 40.9 % error for millet and maize. VV polarisation provides better discrimination between maize and millet with an error of 5.6%, compared with 21.4 % for VH.

V. CONCLUSION

This work explored the ability of Sentinel-1 radar data for crop monitoring in the Sahelian context where agriculture is characterized by small plots and often mixed crops. Such context is not suitable for a straightforward duplication of methods used in other countries. This difficulty has always been a handicap for monitoring crops in the Sahel. However, in recent years, the availability of time series of high spatial resolution images has brought about new interest from scientists. Radar data, unlike optical data, can be adapted to agricultural monitoring in the Sahelian belt. This is because agriculture is almost exclusively rainfed, and during the rainy season, cloud cover is often high, severely limiting the use of optical data.

This study aimed to discriminate three crops (millet, maize and peanuts) from a series of Sentinel-1 radar images, initially seeking to mask non-agricultural areas. A series of fourteen images was used in this study.

The analysis of the temporal profile of different land uses (water, natural vegetation, habitat and bare soil) showed that there is a big difference between agricultural and uncultivated areas at the beginning of the rainy season.

This difference allowed to create a mask of the non-agricultural areas and to concentrate only on the cropped ones.

The analysis of variance (ANOVA) of the three cultures, performed on the time series made it possible to identify and eliminate the non-discriminating data (dates). The prediction model constructed with the data in VV and then VH produced rather large overall errors (47.3% in VV and 40.8% in VH). However, there was a very good ability of Sentinel-1 data to discriminate peanut from other crops with only 16.8% error in VV and 17.2% in VH, which is a big achievement for agricultural monitoring in this part of the world where mapping of crop areas is very difficult. Maize discrimination remained the main limitation of this study. Indeed, given the cultivation practices of maize in this zone (commercial maize sown very early and food corn sown later), it was not easy to discriminate, especially since that difference was not taken into account for the sampling. Therefore, to improve these results it is necessary to differentiate both types of maize crop during the sampling. The use of more advanced discrimination algorithms or prediction models could also help to better analyze the potential of Sentinel-1 radar time series for crop monitoring and mapping in the Sahel.

REFERENCES

[1] Jarlan, L. Inversion des données des diffusiomètres spatiaux pour le suivi de la végétation en zone semi-aride : application au Sahel africain. Thèse de doctorat, Université Paul Sabatier, Toulouse, 2001, 263 p.

[2] Akbari, M.; Mamanpoush, A.R.; Gieske, A.; Miranzadeh, M.; Torabi, M.; Salemi, H. Crop and land cover classification in Iran using Landsat 7 imagery. Int. J. Remote Sens. 2006, 2006, 27, 4117–4135

[3] Fritz, S.; See, L.; Rembold, F. Comparison of global and regional land cover maps with statistical information for the agricultural domain in Africa. Int. J. Remote Sens. 2010, 31, 2237–2256, doi:10.1080/01431160902946598

[4] Vancutsem, C.; Marinho, E.; Kayitakire, F.; See, L.; Fritz, S. Harmonizing and combining existing Land Cover/Land Use datasets for cropland area monitoring at the African continental scale. Remote Sens. 2012, 5, 19–41.

[5] Delrue, J.; Bydekerke, L.; Eerens, H.; Gilliams, S.; Piccard, I.; Swinnen, E. Crop mapping in countries with small-scale farming: A case study for West Shewa, Ethiopia. Int. J. Remote Sens. 2013, 34, 2566–2582, doi:10.1080/01431161.2012.747016.

[6] Lambert, M.J.; Waldner, F; Defourny, P. Cropland Mapping over Sahelian and Sudanian Agrosystems: A Knowledge-Based Approach Using PROBA-V Time Series at 100-m. Remote Sens. 2016, 8, 232; doi:10.3390/rs8030232

[7] Nagai, S.; Saigusa, N.; Muraoka, H.; Nasahara, K.N. What makes the satellite-based EVI–GPP relationship unclear in a deciduous broad-leaved forest? Ecol. Res. 2010, 25359–65

[8] Wu, W.; Shibasaki, R.; Yang, P.; Zhou, Q.; Tang, H. Remotely sensed estimation of cropland in China: A comparison of the maps derived from four global land cover datasets. Can. J. Remote Sens. 2017, 34, 467–479, doi:10.5589/m08-059.

[9] Karkauskaite, P.; Tagesson, T.; Fensholt, R. Evaluation of the plant phenology index (PPI), NDVI and EVI for start-of-season trend analysis of the Northern Hemisphere boreal zone. Remote Sens. 2017, 9485

[10] Le Toan, T.; Paulsader, M.; Flouzat, G.; Fluhr, A. Soil moisture content and microwave backscatter in the 1.5-9 GHZ region. Invited paper, Int. Geosci. Remote Sensing. Symp., Washington, DC, june 1981.

[11] Ulaby, F.T.; Batlivala, P.B.; Dobson, M.C. Microwave backscatter dependence on surface roughness, soil moisture and soil texture: Part I-Bare soil. IEEE Trans. Geosci. Electron. GE-16(4), 1978, p. 286-295.

[12] Bruckler, L.; Witono, H.; Stengel, P. Near surface soil moisture estimation from microwave measurements. Remote sensing. Environment, 1988, 28, p. 101-121

[13] Frison, P.L.; Mougin, E.; Hiernaux, P. Observations and interpretation of seasonal ERS-1 wind scatterometer data over Northern Sahel (Mali). Remote Sensing of Environment, 1998, 693, 233– 242.

[14] Jarlan, L.; Mougin, E.; Frison, P.L.; Mazzega, P.; Hiernaux P. Analysis of ERS wind scatterometter time series over Sahel (Mali). Remote Sensing of Environment, 2002, 81, 404-415.

[15] Zine, S. Contribution de la télédétection satellitale radar pour le suivi des paramètres de surface d'une zone sahélienne agro-pastorale, thèse de doctorat de l'Université de Marne-la-Vallée, 2004.

[16] Calvet, J.C.; Wigneron, J.P.; Walker, J.; Karbou, F.; Chanzy, A.; Albergel, C. Sensitivity of passive microwave observations to soil moisture and vegetation water content: L-band to W-band. IEEE Trans. Geosci. Remote Sens. 2011, 49:1190–1199. doi:10.1109/TGRS.2010.2050488

[17] Faye, G.; Frison, P.L.; Diouf, A.A.; Wade, S.; Kane, C.A.; Fussi, F.; Jarlan, L.; Niang, F.K.N.; Ndione, J.A.; Mougin, E. Soil estimation in the Ferlo region (Senegal) using Radar Envisat/ASAR and Optical Spot/Vegetation data. Egyptian Journal of Remote Sensing Space Sci, 2017, 21 (2018) S13–S22

[18] Bousbih, S.; Zribi, M.; Lili-Chabaane, Z.; Baghdadi, N.; El Hajj, M.; Qi Gao.; Mougenot, B. Potential of Sentinel-1 Radar Data for the Assessment of Soil and Cereal Cover Parameters. Sensors 2017, 17, 2617; doi:10.3390/s17112617

[19] MEPN. Schéma directeur de la zone éco-géographique sylvopastorale, Sénégal, 1999, 20 pages.

[20] Tostain, S. Le mil, une longue histoire : hypothèses sur sa domestication et ses migrations. Plantes et Paysages d'Afrique, 1998, 461–490.

[21] Bezançon, G.; Pham, J.L. Ressources génétiques des mils en Afrique de l'Ouest : Diversité, conservation et valorisation. (G. Bezançon & J. L. Pham, Eds.). IRD Editions, 2004.

[22] Hamon, P. Diversité génétique des plantes tropicales cultivées. Editions Quae, 1999.

[23] Brink, M.; Belay, G.M. Ressources végétales de l'Afrique tropicale 1. Céréales et légumes secs. (M. Brink & G. Belay, Eds.). Fondation PROTA / Backhuys Publishers / CTA, Wageningen : Pays-Bas, 2006.

[24] Durovray, J. L'amélioration variétale du maïs au Sénégal. Agronomie Tropicale XXXI-3, XXVIII, 1976, 259-264 .

[25] Mémento de l'agronome, F. M. des affaires étrangères. Mémento de l'agronome. (F. M. des affaires Étrangères, Ed.). Editions Quae, 2002.

[26] Chevalier, A. L'origine botanique et l'amélioration des Arachides cultivées. Essai d'une classification systématique. Revue de Botanique Appliquée et D'agriculture Coloniale, 1929, 9(90), 97–102

[27] Gillier, P.; Silvestre, P. L'ARACHIDE. G.-P. Moisonneuve et Larose, 1969.

[28] Copernicus Open Data Hub. Available online: https://sentinel.esa.int/web/sentinel (accessed on mars 2017).

[29] Baup, F.; Mougin, E.; De Rosnay, P.; Timouk, F.; Chênerie, I. Surface soil moisture estimation over the AMMA Sahelian site in Mali using ENVISAT/ASAR data. Remote Sensing of Environment, 2007, 109 (2007) 473–481

[30] Breiman, L.; Friedman, R.A.; Olshen, R.A.; Stone, C.G. Classification and Regression Trees. Pacific Grove, CA: Wadsworth, 1984.

[31] Salford-Systems, 2001. Classification and regression trees a robust decision-tree technology for data mining, predictive modelling and data processing. San Diego, USA, 2001, p.335.

[32] Faye, G.; Frison, P.L.; Wade, S.; Ndione, J.A.; Beye, A.C.; Rudant, J.P. Etude de la saisonnalité des mesures des diffusiomètres SCAT : apport au suivi de la végétation au Sahel, cas du Ferlo au Sénégal. Télédétection, 2011, Vol. 10, No. 1, pp. 23–31.

[33] Frison, P.L.; Mougin, E. Monitoring global vegetation dynamics with ERS-1 wind-scatterometer data, International Journal of Remote Sensing, 1996, 17, pp. 3201-3218.

[34] Jarlan, L.; Mazzega, P.; Mougin, E.; Lavenu, F.; Marty, G.; Frison, P.L. Mapping of Sahelian vegetation parameters from ERS scatterometer data with an evolution strategies algorithm. Remote Sensing of Environment, 2003, 87, 72−84.

[35] Mattia, M.; Toan, T.L.; Souyris, J.C.; Carolis, G.D.; Floury, N.; Posa, F.; Pasquariello, G. The effect of surface roughness on multifrequency polarimetric SAR data. IEEE Trans. Geosci. Remote Sens. 1997, 35, 954–966

[36] Calvet, J.C., Wigneron, J.P.; Walker, J.; Karbou, F.; Chanzy, A.; Albergel, C. Sensitivity of passive microwave observations to soil moisture and vegetation water content: L-band to W-band. IEEE Trans. Geosci. Remote Sens, 2011, 49:1190–1199. doi:10.1109/TGRS.2010.2050488

[37] Zribi, M.; Gorrab, A.; Baghdadi, N.; Lili-Chabaane, Z.; Mougenot, B. Influence of radar frequency on the relationship between bare surface soil moisture vertical profile and radar backscatter. IEEE Geosci. Remote Sens. Lett. 2014, 11, 848–852.

[38] Alexakis, D.D.; Mexis, F.K.; Vozinaki, A.K.; Daliakopoulos, I.N.; Tsanis, I.K. Soil Moisture Content Estimation Based on Sentinel-1 and Auxiliary Earth Observation Products. A Hydrological Approach. Sensors 2017, 17, 1455

[39] Baghdadi, N.; Zribi, M.; Bruand, A.; King, C. Potentiel of ASAR/ENVISAT for the characterization of soil surface parameters over bare agricultural fields. Sensors 2010, 10, 8899–8900.